The effect of sulfur on the glass transition temperature in anorthite-diopside eutectic glasses

Yann Morizet, S Ory, Ida Di Carlo, Bruno Scaillet, Patrick Echegut

▶ **To cite this version:**

Yann Morizet, S Ory, Ida Di Carlo, Bruno Scaillet, Patrick Echegut. The effect of sulfur on the glass transition temperature in anorthite-diopside eutectic glasses. Chemical Geology, 2015, 416, pp.11-18. 10.1016/j.chemgeo.2015.10.010 . insu-01225168

HAL Id: insu-01225168

https://insu.hal.science/insu-01225168

Submitted on 5 Nov 2015

HAL is a multi-disciplinary open access archive for the deposit and dissemination of scientific research documents, whether they are published or not. The documents may come from teaching and research institutions in France or abroad, or from public or private research centers.

L'archive ouverte pluridisciplinaire **HAL**, est destinée au dépôt et à la diffusion de documents scientifiques de niveau recherche, publiés ou non, émanant des établissements d'enseignement et de recherche français ou étrangers, des laboratoires publics ou privés.

Distributed under a Creative Commons Attribution - NonCommercial - NoDerivatives 4.0 International License

Accepted Manuscript

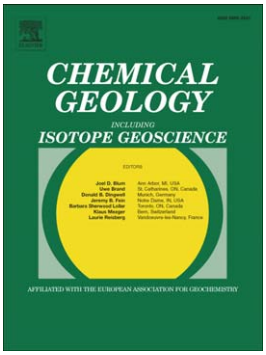

The effect of sulfur on the glass transition temperature in anorthite-diopside eutectic glasses

Y. Morizet, S. Ory, I. Di Carlo, B. Scaillet, P. Echegut

PII: S0009-2541(15)30057-7
DOI: doi: 10.1016/j.chemgeo.2015.10.010
Reference: CHEMGE 17719

To appear in: *Chemical Geology*

Received date: 20 May 2015
Revised date: 7 September 2015
Accepted date: 5 October 2015

Please cite this article as: Morizet, Y., Ory, S., Di Carlo, I., Scaillet, B., Echegut, P., The effect of sulfur on the glass transition temperature in anorthite-diopside eutectic glasses, *Chemical Geology* (2015), doi: 10.1016/j.chemgeo.2015.10.010

This is a PDF file of an unedited manuscript that has been accepted for publication. As a service to our customers we are providing this early version of the manuscript. The manuscript will undergo copyediting, typesetting, and review of the resulting proof before it is published in its final form. Please note that during the production process errors may be discovered which could affect the content, and all legal disclaimers that apply to the journal pertain.

ACCEPTED MANUSCRIPT

THE EFFECT OF SULFUR ON THE GLASS TRANSITION TEMPERATURE IN ANORTHITE-DIOPSIDE EUTECTIC GLASSES.

Y. MORIZET[1,2,*], S. ORY[3], I. DI CARLO[1], B. SCAILLET[1], P. ECHEGUT[3]

[1] Institut des Sciences de la Terre D'Orléans (ISTO) UMR 7327, CNRS -Université d'Orléans-BRGM, Campus Géosciences, 1A rue de la Férolerie, 45071 ORLEANS Cedex 2

[2] Laboratoire de Planétologie et Géodynamique de Nantes (LPGN) UMR CNRS 6112, Université de Nantes, Nantes Atlantique Universités, 2 rue de la Houssinière, 44322 NANTES (France)

[3] CNRS, CEMHTI UPR3079, Université d'Orléans, F-45071 ORLEANS (France)

Corresponding author: Dr Yann Morizet

Permanent address:

Laboratoire de Planétologie et Géodynamique de Nantes (LPGN), Université de Nantes

CNRS/INSU – UMR CNRS 6112

2 rue de la Houssinière, BP 92208.

44322 Nantes Cedex 3 (FRANCE).

Email: yann.morizet@univ-nantes.fr

Tel: +33 (0) 2 5112 5491

Fax: +33 (0) 2 5112 5268

ACCEPTED MANUSCRIPT

ACCEPTED MANUSCRIPT

Abstract:

The effect of sulfur dissolved in anorthite-diopside eutectic (AD) glasses on the glass transition temperature (Tg) has been investigated via Differential Scanning Calorimetric measurements (DSC) and Thermogravimetric Analysis (TGA) under moderately reducing to oxidizing conditions.

In a series of AD glasses, we have measured the change in Tg as a function of S content present as SO_4^{2-} (HS^- is also identified to a lesser extent) and H_2O content. The AD glasses investigated have S contents ranging from 0 to 7519 ppm and H_2O contents ranging from 0 to 5.3 wt.%. In agreement with previous studies, increasing H_2O content induces a strong exponential decrease in Tg: volatile free AD glass has a Tg at 758±13°C and AD glass with 5.18±0.48 wt.% H_2O has a Tg at 450±11°C. The change in Tg as a function of H_2O is well-reproduced with a third-order polynomial function and has been used to constrain Tg at any H_2O content. The effect of S on Tg is almost inexistent or towards a decrease in Tg with increasing S content. For instance, at ~2.4 wt.% H_2O, the addition of S induces a change in Tg from 585±10°C with 0 ppm S to 523±3°C with 2365±138 ppm S; a further increase in S up to 7239±90 ppm S does not induce a dramatic change in Tg measured at 529±2°C.

The limited effect of S on the glass transition temperature contrasts with recent spectroscopic measurements suggesting that S dissolution as SO_4^{2-} groups provokes an increase in the polymerization degree. We propose an alternative view which reconciles the spectroscopic evidence with the Tg measurements. The dissolution of S as SO_4^{2-} does not induce the formation of Si-O-Si molecular bonding through consumption of available non-bridging oxygens (NBO) but instead we suggest that Si-O-S molecular bonds are formed which are not detectable by DSC measurements but mimic the increase in glass polymerization. Therefore,

ACCEPTED MANUSCRIPT

spectroscopic measurements must be used with caution in order to extract melt physical properties.

Number of words: 324

Keywords: glass transition temperature, calorimetric measurements, silicate glass, sulfur dissolution mechanisms.

ACCEPTED MANUSCRIPT

ACCEPTED MANUSCRIPT

1. Introduction:

Sulfur (S) is an important volatile element implied in volcanic system (Carroll and Webster, 1994; Paris et al., 2001; Scaillet et al., 2003; Clemente et al., 2004; Scaillet and Pichavant, 2005; Moune et al., 2009), playing a major role in degassing processes and related atmospheric changes (Carroll and Webster, 1994; Edmonds et al., 2003; Webster and Mandeville, 2007; Oppenheimer et al., 2011). The behaviour of S in magmas is complex owing to its variable oxidation state in silicate melts: under oxidising conditions S is present as sulfate groups (SO_4^{2-} where sulfur is S^{6+}), whilst under reducing conditions S is present as sulphide groups (where sulfur is S^{2-}) (e.g. Fincham and Richardson, 1954; Carroll and Rutherford, 1988; O'Neill and Mavrogenes, 2002; Jugo et al., 2005a,b; Moretti and Ottonello, 2005; Klimm and Botcharnikov, 2010; Baker and Moretti, 2011; Klimm et al., 2012).

The structure of a silicate glass can be described via a model involving Q-species (e.g. Grimmer et al., 1984; Brandiss and Stebbins, 1988; Merzbacher et al., 1990; Stebbins, 1995; Mysen and Richet, 2005). A Q^n unit represents a tetrahedral structural unit with n bridging oxygens (BO, n = 0 to 4). The abundance of each Q^n species is dependent on bulk composition (e.g. Maekawa et al., 1991; Mysen and Frantz, 1993; Frantz and Mysen, 1995; Malfait et al., 2007). The distribution of those individual Q-species can be related to the structure of melts, hence to their physical properties such as viscosity (e.g. Mysen et al., 1980; Mysen, 1998; Toplis and Dingwell, 2004; Neuville, 2006; Malfait et al., 2007).

The presence of volatile species influences the distribution of Q-species in silicate glasses. For instance, H_2O induces a strong melt depolymerisation when dissolving as OH groups (e.g. Farnan et al., 1987; Kummerlen et al., 1992; Zotov and Keppler, 1998; Zeng et al., 1999; Xue and Kanzaki, 2004, 2008; Mysen and Cody, 2005; Xue, 2009) according to the following general reaction:

ACCEPTED MANUSCRIPT

$$Si-O-Si+H_2O \leftrightarrow 2Si-O-H \qquad \text{Eq. 1}$$

In this dissolution mechanism, a water molecule breaks the bridge between two Q^n structural units changing, therefore, Q^n species into Q^{n-1}, less polymerised, species. Because molecular bonding is broken during this process, it impacts the melt physical properties such as viscosity. This common water dissolution mechanism is not the only one occurring in silicate melt and other dissolution mechanisms have been proposed. For instance, in highly depolymerized melt, water has been suggested to have an opposite effect, it induces an increase in the degree of polymerization (Romano et al., 2001; Xue and Kanzaki, 2004; Moretti and Ottonello, 2005; Giordano et al., 2009; Malfait and Xue, 2014).

Viscosimetric measurements on hydrous silicate melt (e.g. Scaillet et al., 1996; Richet et al., 1996; Whittington et al., 2000; Giordano and Dingwell, 2003; Robert et al., 2013) as well as glass transition temperature (Tg used as a proxy for viscosity) determination in hydrous silicate glasses (e.g. Deubener et al., 2003; Giordano et al., 2005; Morizet et al., 2007) confirm this fact. It is also consistent with the possible structural definition of glass transition temperature. The glass transition temperature is a temperature corresponding to a fixed relaxation time of the silicate melt structure which is thought to correspond to the exchange rate of the oxygens between tetrahedral units (Moynihan et al., 1976; Liu et al., 1988; Moynihan, 1995). As a result, there is a direct correlation between the change in the degree of polymerisation induced by H_2O dissolution and the diminution in Tg value observed with increasing H_2O content (Dingwell et al., 1996; 1998; Giordano et al., 2008a,b).

In contrast to water, the effect of sulfur on viscosity or Tg is currently unknown. Recent spectroscopic investigations by Morizet et al. (2013) lead to the proposition that the presence of SO_4^{2-} induces an apparent polymerisation of the melt which could therefore translate into an increase in melt viscosity or an increase in Tg. Whether this increase in polymerisation

ACCEPTED MANUSCRIPT

corresponds to an increase in glass transition temperature involving the formation of Si-O-Si molecular bonding is yet not clear. Morizet et al. (2013) suggested that the dissolution of S as SO_4^{2-} is accompanied by the formation of Si-O-S (their equation 9) and hence might not be viewed as a true polymerization process.

In the present study, we investigated the change in Tg in anorthite-diopside eutectic glasses (AD) with known S and H_2O contents, similar to those investigated in Morizet et al. (2013). In the studied AD glasses S is dissolved mainly as SO_4^{2-} but also as HS^-, though in minor amounts. The choice for this composition is motivated by the fact that the obtained calorimetric results can be compared to both the spectroscopic of Morizet et al. (2013) and to viscosity and Tg data obtained by Giordano et al. (2008a) on the same anorthite-diopside eutectic composition with various H_2O content. The results are discussed in terms of the effect of S and H_2O on Tg and the way sulfur dissolves into the silicate melt structure is also discussed.

2. Experimental and analytical methods:

2.1. Experimental method:

In the present study, we used the quenched glass samples investigated in Morizet et al. (2013) and additional glass samples were also synthesised. The dataset produced by Morizet et al. (2013) consists in glasses of anorthite-diopside eutectic composition (50.2 SiO_2, 15.7 Al_2O_3, 23.4 CaO and 10.6 MgO in wt.%). From a theoretical standpoint, the investigated glass composition is slightly depolymerised with an NBO/T close to 0.9 (i.e. NBO/T can have values from 0 to 4) using the method of Mysen (1988, 1990). The detailed glass compositions are provided in the Supplementary material and in Table 1. The starting composition preparation method is fully described in Morizet et al. (2013) and in most of the case it

ACCEPTED MANUSCRIPT

consists in mixing a starting volatile-free AD glass powder (ADVF in Table 1) with a known amount of elemental S (0 to ~5 wt.%, see Table 1). Prior to loading the obtained mixture into the Pt capsule a known amount of H_2O (up to 8.2 wt.% H_2O) is loaded at the bottom of the capsule using a micro syringe. For three samples (AD5M-2, AD2M-5 and AD10M-5) we adopted the method described in Zajacz (2015) who used a sulphuric acid solution with a known S concentration instead of elemental S as a source of S. For those samples, solutions with 2, 5 and 10 mol.L^{-1} of H_2SO_4, corresponding to 0.25, 0.7 and 1.6 wt.% S, were loaded into the charge (~3.5 wt.% H_2O).

As shown in Table 1, the AD glasses were synthesised at 300 MPa using an Internally Heated Pressure Vessel (IHPV) at 1250°C with a quench rate above 150°C/s. (Di Carlo et al., 2006). Most of the glasses were synthesised under oxidizing conditions (using only Ar as pressurizing gas, which yields an intrinsic fH_2 of the IHPV of 1.0-1.4 bars); however, some AD glass samples were also synthesised under moderately reducing conditions: AD20 to AD24. Those experiments were conducted with an IHPV at 300 MPa and 1250°C with a fH_2 of either 3 bars (AD20 to AD22) or of 10 bars (AD23 and AD24), which were produced using an Ar-H2 mixture. Five additional samples were synthesised using piston cylinder apparatus at 500 MPa and 1450°C. For these experiments we used a ¾ inch pressure plate with a special design (Morizet et al., 2015) which allows quench rate higher than usually observed with that kind of apparatus (on the order of 200°C/s.). Therefore, it can be considered that glasses synthesised using either IHPV or piston-cylinder apparatus have a comparable thermal history (i.e. quench rate) and that the small difference in quench rate is unlikely to produce any noticeable changes on Tg (Webb and Dingwell, 1990; Dingwell, 1995). The piston cylinder experiments run duration was kept short (2h) in order to avoid substantial H diffusion through the capsule walls which could lead to a possible reduction of the charge (Matjuschkin et al., 2015).

ACCEPTED MANUSCRIPT

The fO_2 conditions during the IHPV experiments are calculated using the H_2O content measured in the glass and the prevailing fH_2 (fH_2 conditions in piston cylinder experiment is unknown). The calculated fO_2 for each sample is reported in Table 1 and is expressed relative to FMQ. ADVF sample was synthesised in air which corresponds to ΔFMQ+5. The moderate fO_2 conditions applied (ΔFMQ+2.8 to +0.8) did not induce a significant change in S speciation, as shown in Table 1. Only a few samples show the existence of reduced S species (HS^-) as identified with a peak located at ~2575 cm^{-1} (Klimm and Botcharnikov, 2010; Klimm et al., 2012) from Micro-Raman spectroscopy. In sample AD-5-5, 3% of HS^- is identified and considered as negligible. Typical example of Raman spectra are provided in the Supplementary material. The small fraction of HS^- in spite of moderate reducing condition is consistent with Fe-free experimental work pioneered by Nagashima and Katsura (1973) showing that in Fe-free glass compositions, the HS^- species appears below ΔFMQ+2.

2.2. Volatile content measurements:

The reader is referred to Morizet et al. (2013; their section 3.1 and 3.3) for a full description of the methods used to measure volatile content in the recovered glasses. The major element chemical composition and the S content have been determined by Electron Probe Micro Analysis (EPMA). More than 20 point analyses were acquired to obtain a representative standard deviation in the S content (see Table 1). One interesting point to notice is that the measured S content appears to be maximised when the experimental protocol uses H_2SO_4 aqueous solution as the initial source for S. For instance, AD2M-5 and AD5M-2 were synthesised with an initial S content of 0.25 and 0.7 wt.% S, respectively; the measured S content for those samples is 2365±138 and 7239±90 ppm, respectively. On the contrary, charges prepared with elemental S have a measured S content which is well-below the initial loaded S content (see Table 1). For example, AD12 has ~5 wt.% as an initial S content and

ACCEPTED MANUSCRIPT

the measured S content in the glass is less than 1000 ppm. In the current, it is not clear if this behaviour is dependent on the initial H_2O content. The enhanced capability of S dissolution when S is loaded in the experimental charge as an aqueous sulphuric solution has been pointed out by Zajacz (2015).

We used FTIR spectroscopy and followed the method described in Morizet et al. (2013) to determine the total water content (H_2O^{tot}). For the newly synthesised glass samples, a 256 scans collection was done to obtain a good signal-to-noise ratio. We used an IR light source, a MCT-B detector and a CaF_2 beamsplitter as a spectrometer configuration. The water content was determined by summing up the contribution of OH^- and H_2O^{mol} vibrations peaks located at 4500 and 5200 cm^{-1}, respectively. The concentration of each water species was calculated with the Beer-Lambert approximation using the peak areas and the integrated molar absorption coefficients (ε). As explained in Morizet et al. (2013), the integrated extinction coefficients from Stolper (1982) (200 and 300 $L.mol^{-1}.cm^{-2}$ for OH^- and H_2O^{mol}) for a An-Di like composition need a correction factor (x1.6) in order to retrieve correct H_2O concentrations. Therefore, we used $\varepsilon OH^- = 125$ $L.mol^{-1}.cm^{-2}$ and $\varepsilon H_2O^{mol} = 187.5$ $L.mol^{-1}.cm^{-2}$. The H_2O^{tot} in the studied glasses ranges from 1.03 to 5.33 wt.% for AD1H-6 and AD23, respectively. The typical error on water measurement is better than 0.5 wt.% (see Table 1).

2.3. DSC-ATG measurements:

We used differential scanning calorimeter (DSC SETSYS EVO 2400) equipped with a thermogravimetric analyser (TGA). The glass transition temperature (Tg) for each recovered glass sample was determined using the variation of heat flow (in mW) with increasing temperature (Py et al., 2011). Prior to the sample analysis, the heat flow from two identical

ACCEPTED MANUSCRIPT

empty Pt-Rh crucibles (6 mm in diameter) was measured to determine the baseline of the DSC apparatus, which was subtracted from the standard and sample measurements. The DSC was then calibrated by measuring the enthalpy of fusion of metal standards (gold, silver, aluminium and nickel) and the sensitivity is better than 0.5% in relative with respect to the temperature measurement. Additional TGA measurements were also conducted conjointly to DSC measurements in order to determine the possible volatile loss during the heating cycle for determining the glass transition temperature.

Prior to calorimetric measurements, the glass samples were crushed to avoid sample fragmentation during the DSC experiment. The crushed glass was placed in one of the crucibles and its heat flow was measured. All measurements were performed with the same two crucibles under a constant flow of Ar gas of 20 $ml.min^{-1}$. Each sample was heated from 40°C across the glass transition at a rate of 10 or 20 K/min (see Table 2). The glass transition temperature is characterised by a decrease in the heat flow (as shown in Figure 1). In the liquid state (above Tg) there is a constant decrease in the heat flow followed by a strong increase around 700°C. This change in the heat flow curve shape with increasing temperature may be attributed to crystallization of the sample. For these samples further repeated measurements (after controlled cooling) is not possible as the sample's aspect had clearly changed due to crystallization.

1. Results:

1.1. Tg determination from DSC curves:

The Tg value was determined by the in-built DSC software (Setsoft 2000) using the tangent definition as shown in Figure 1A for AD-5-3 sample DSC measurement. Tg is defined by the three points definition. Two tangents with the same slope coefficient are fitted before and after the glass transition region. A third tangent is fitted on the glass transition region curve.

ACCEPTED MANUSCRIPT

The Tg value is represented by the mid-point of this last segment defined by the intersection obtained with the two tangents before and after the glass transition region. The used Tg value corresponds to the typical inflection point definition and is different to the Tg defined by the onset temperature (Mazurin, 2007). The Tg temperature defined by the onset point is lower in value as compared to the inflection point. We have estimated this difference using the heat flow curves obtained on our investigated samples. On average the Tg defined by the tangent method is higher by 20°C as compared to the Tg defined by the inflection point (see Supplementary material for both Tg values).

Based on the reproducibility of the Tg measurements, we suggest a large uncertainty (±5 K) associated with the Tg determination. This error is larger than it is usually assumed for that kind of apparatus (±2.5 K, Giordano et al., 2005; Morizet et al., 2007). The replicate measurements conducted on several samples (see Table 2, ADVF and AD-5-0) yield an uncertainty larger than the suggested ±5 K and on the order of ±10 K which is still a low error considering the observed large change in Tg values (more than 250 K). Replicated measurements were also conducted with different heating rates (10 or 20 K/min, see Table 2). For AD-5-3, changing the heating rate does not result in a change in the determined Tg as shown in Fig. 1B: changing the heating rate between 10 and 20 K/min results in a Tg variation of less than 5 K. This result is consistent with previous works suggesting that Tg is a function of thermal history (Giordano et al., 2005; Morizet et al., 2007). However, the change in Tg appears to be close to the asserted uncertainty in Tg measurements. We, therefore conclude that Tg determination can be readily compared regardless of the used heating rate.

The rapid rise in the heat flow, indicating possible crystallization or foaming, occurs at higher temperatures than Tg. Considering that Tg marks the beginning of the relaxation process, the

ACCEPTED MANUSCRIPT

timescales of structural relaxation are too long for volatile escape at this point. This is supported by diffusion calculations using the equations of Freda et al. (2005). At such a low temperature (<600°C) the S diffusive loss is insignificant and does not exceed the μm scale. Moreover, we have conducted combined TGA and DSC measurements to investigate the possibility for diffusive loss below the Tg. We represent the combined DSC and TGA for four samples in Figure 2. We observe clearly that any loss in mass occurs well-above the Tg value (>600°C) supporting the view that the dissolved volatiles (S and H_2O) do not escape the glass sample below Tg.

An additional feature can be observed from typical DSC curves shown in Figure 3. The position of the Tg is indicated by the dot on the curve. There is an unambiguous change in the Tg value in between the samples (see also Table 2 for the whole set of determined Tg values). However, we observe an additional peak located well-below the determined Tg. This peak is also observed in Figure 1B in replicated measurements for AD-5-3 and also visible in Figure 2A for AD-5-0 DSC curve. For instance, this peak is located at ~ 425°C and 360°C for AD-5-3 and AD-4.5-1 (less visible), respectively. This peak is currently unexplained, however, it is observed in both S-free and S-rich samples. The characterization of the glass samples by Morizet et al. (2013) revealed that the glass samples contained $H_2O+SO_2\pm H_2S$ fluid inclusions. Thus, the 300-400°C peak could arise from the burst of residual fluid inclusions in the glass powder whenever the glass samples were not finely crushed. Alternatively, it could correspond to an instrumental artefact. In any case, we believe that it does not influence the Tg position and determination owing to 1) the large interval between the Tg value and this feature (more than 100°C) and 2) the way Tg is defined by the two tangents method (the slope of the tangents is not affected by this feature).

ACCEPTED MANUSCRIPT

1.2. Effect of volatiles content on glass transition temperature:

The determined Tg values as a function of volatile contents are shown in Figure 4: Figure 4A as a function H_2O content and Figure 4B as a function of S content. In both plots we added either the ppm S or wt.% H_2O next to each data point. As a function of H_2O, most of the determined Tg values define an exponential decay trend. The S- and H_2O-free sample (ADVF) exhibits the highest Tg value at 767°C whereas the sample with the highest H_2O content and S-free (AD-5-0) has the second lowest Tg value at 450°C. Such a negative trend for Tg with increasing H_2O is consistent with previous studies obtained on various types of glass compositions, based on either viscosimetric or Tg calorimetric measurements (e.g. Dingwell et al., 1996, 1998; Whittington et al., 2000, 2001; Deubener et al., 2003; Giordano et al., 2004, 2005; Di Genova et al., 2013; Robert et al., 2013, 2014). It also supports the model for water dissolution mechanism in silicate inducing a strong depolymerisation of the melt through Si-O-Si bond breaking (e.g. Farnan et al., 1987; Kummerlen et al., 1992; Zotov and Keppler, 1998; Zeng et al., 1999; Mysen and Cody, 2005) and therefore the decrease in Tg value.

We have tried to apply existing models which take into account the effect of H_2O and chemical composition. The change in Tg as a function of H_2O content for a theoretical anorthite-diopside eutectic composition has been calculated using the general model of Giordano et al. (2008b; dashed line in Figure 4A) and the model of Giordano et al. (2008a; dotted line in Figure 4B) applied to anorthite-diopside join. It should be mentioned that in both models, Tg is calculated at the onset which represents a lower value as compared to the Tg we derive from the tangent method. However, as explained earlier, the difference in between the value is not significant (~20°C). Both models seem to bracket the measured Tg values. However, considering the data point distribution as well as the repartition of the S-free H_2O-bearing points, Giordano et al. (2008a) is more adequate to reproduce our Tg data

ACCEPTED MANUSCRIPT

than the Giordano et al. (2008b), in agreement with the fact that Giordano et al. (2008a) has been calibrated on identical glass compositions to the one studied here. Furthermore, considering a 20°C decrease in the measured Tg so as to correspond to the onset Tg will provide an even better agreement with the model of Giordano et al. (2008a).

In contrast, the change in Tg as a function of S content is more difficult to constrain. In Figure 4A, it appears that the measured Tg for almost all S-bearing glasses is very close to the Tg value predicted by the model of Giordano et al. (2008a) which only considers the effect H_2O which suggests that S does not affect significantly glass transition temperature. It should be emphasised that this is in sharp contrast with the spectroscopic interpretation from Morizet et al. (2013). This aspect will be further discussed in section 4.2. The absence of S effect on Tg can only be approached at a constant water content. For instance, S-free AD-3-0 exhibits a Tg value at 545°C with 3.01 wt.% H_2O while AD-4.5-1 exhibits a Tg value at 504°C with 3.1 wt.% H_2O and 4150 ppm S. This difference in Tg value (ΔTg = 41°C) is largely beyond error in Tg determination. We note that at such a high H_2O content, a variation of 0.1 wt.% H_2O produces a change in Tg of about 10°C (see Giordano et al., 2005; Whittington et al., 2009). This observation points towards a negative effect of S dissolved as SO_4^{2-} on Tg which conflicts again with previous spectroscopic-based inferences by Morizet et al. (2013).

We also added in Figure 4B horizontal lines corresponding to the calculated Tg values at a fixed H_2O contents (2.0, 3.0 and 4.0 wt.%) using Giordano et al. (2008a) model. This approach suggests an absence of any strong S effect on Tg. At 2.0 wt.% H_2O, the model gives Tg = 551°C; AD10M-5 with 2.0 wt.% H_2O and 5481±324 ppm S has a measured Tg = 544±5°C. At 3.0 wt.% H_2O, the model gives Tg = 503°C; AD4 and AD-4.5-1 at 3.1 wt.% H_2O have a measured Tg = 507 and 504±5°C for 2718±598 and 4150±974 ppm S,

ACCEPTED MANUSCRIPT

respectively. Within error the measured Tg values are almost identical to the predicted Tg value by the model therefore suggesting that S does not influence Tg.

2. Discussion:

2.1. Model for the effect of S on Tg:

We tested several mathematical functions in order to quantify the effect of both H_2O and S on Tg. The Tg data are reproduced as a function of both H_2O and S on a molar fraction basis with the following function:

$$Tg(H_2O,S) = 426 + 325 \times e^{(-14.2\,XH_2O)} - 2594\,XS + 286869\,XS^2 \qquad \text{Eq. 2}$$

The measured Tg versus the calculated Tg values are reported in Figure 5: in Figure 5A Tg is calculated with the model of Giordano et al. (2008a) and in Figure 5B Tg is calculated with Eq. 2. The correlation factor (r^2) is 0.914 and 0.921 with the linear regression in Figure 5A and 5B, respectively. The error on the calculated Tg value using Eq. 2 is derived from linear regression and does not exceed ±19°C. In Eq. 2, the negative value of the parameter associated with the XS witnesses a negative effect of S on Tg. This negative effect remains trivial considering 1) the exponential form of the Tg dependency as a function of H_2O content and 2) the range of volatile contents usually observed in natural volcanic glasses (i.e. wt.% H_2O versus x100 ppm S). For example, Métrich and Clocchiatti (1996) reported up to 0.34 wt.% S dissolved in melt inclusions from Etna (Italy); De Hoog et al. (2001) reported up to 0.29 wt.% S dissolved in melt inclusions from Galunggung (Indonesia). In general, it appears unlikely that the S content could overwhelm that H_2O content in natural basaltic magmas (e.g. Spillaert et al., 2006). In any case, the presence of S does not induce a dramatic change in the glass transition temperature; hence, melt viscosity might not be strongly affected by the presence of S on the contrary to H_2O.

ACCEPTED MANUSCRIPT

2.2. Implications for S dissolution mechanisms:

The observations reported here are a follow-up of the spectroscopic investigation of Morizet et al. (2013). In their work, Morizet et al. (2013) suggested that S dissolution as SO_4^{2-} groups in silicate melt induces a polymerization of the silicate melt network. The present results based on DSC calorimetric measurement do not support such an effect. The apparent contradiction between NMR and DSC results can be solved by considering the molecular configuration of the SO_4^{2-} groups when dissolving in silicate melt structure. As already stated in the introduction, Morizet et al. (2013) proposed that SO_2 dissolution mechanisms in silicate melts lead to the formation of Si-O-S molecular bonds. On the basis of the above results, we suggest that this cannot be considered as a polymerization process but instead the apparent polymerization observed by ^{29}Si NMR is an analytical artefact. In fact the formation of the Si-O-S is strong enough to change the ^{29}Si NMR spectral signature so as to mimic a polymerization effect of SO_2 dissolution onto the melt structure. In other words, the shift of -3 ppm in the ^{29}Si peak maximum witnessing the apparent increase in melt polymerization only reflects the consumption of non-bridging oxygen by SO_2 molecules to form SO_4^{2-} molecular groups (Manara et al., 2007; Machacek et al., 2010). Consequently, the dissolution of SO_2 molecules in silicate melts does not induce the formation of Si-O-Si bonds, which should be accompanied by an increase in glass transition temperature which is related to the kinetic rate of forming/breaking of Si-O-Si bonds (Liu et al., 1988; Moynihan, 1995).

The potential slight decrease in Tg with increasing S evidenced by fit parameters of Eq. 2 is more difficult to explain as it implies that Si-O-Si molecular bonding are broken upon S dissolution which is unlikely (Machacek et al., 2010). If S dissolution does induce major changes on the silicate network structure, an alternative explanation is that the dissolution of S as SO_4^{2-} induces slight geometrical changes (Si-O bond length and/or angle). Those

ACCEPTED MANUSCRIPT

changes would be important enough to change the configurational entropy (S_{conf}) of the melt according to the Adam-Gibbs theory (Adam and Gibbs, 1965):

$$\ln \eta = A_e + \frac{B_e}{TS_{conf}} \qquad \text{Eq. 3}$$

In Eq. 3, Ae and Be are constants. At a constant viscosity value $\eta = 10^{12}$ Pa.s corresponding to the viscosity at Tg, a decrease in Tg value will be accompanied by an increase in S_{conf}. This point has to be investigated in more details with additional spectroscopic investigation or viscosimetric measurements on S-bearing aluminosilicate glasses.

3. Summary:

In the present study, we have determined the glass transition temperature of anorthite – diopside eutectic glasses synthesised at high pressure and high temperature conditions and equilibrated with H_2O and S present as SO_4^{2-} groups. We have shown that 1) water induces an exponential decrease in Tg in agreement with previous studies and 2) S dissolved as SO_4^{2-} has a limited effect on Tg or slightly decrease Tg. The slight decrease in Tg with increasing S content is in contradiction with spectroscopic based interpretations which suggest that S would induce an increase in glass transition temperature. We explain this discrepancy through the Si-O-S molecular groups which are formed. Those molecular groups induce spectroscopic changes which mimic melt polymerization. The slight decrease in Tg is on the contrary thought to reflect structural geometrical changes inducing changes in thermodynamic configuration properties.

The present work is only preliminary and further work is required in order to obtain a broader picture on the effect of S on melt viscosity. In particular, the role of volatiles species relationship might also be important to look at. Recent work by Baasner et al. (2013) showed

ACCEPTED MANUSCRIPT

that Cl induce an increase in peralkaline melt viscosity. Botcharnikov et al. (2004) showed that there is a strong relationship in between S and Cl in magmatic systems. It would therefore be interesting to address in greater details the possible interactions between different volatile species onto melt viscosity. Considering that it is currently assumed that H_2O produces two different effects on the silicate melt structure: 1) depolymerizing effect in relatively polymerized melt composition or 2) polymerizing effect highly depolymerized melt composition; it might be interesting to determine the change in Tg for various S-bearing melt compositions.

Acknowledgements:

The authors are grateful to the CNRS INSU which financed the current work through the ALEAS program. The authors thank the University of Orléans, the University of Nantes and the CEMHTI for their access to analytical facilities. We thank D.B. Dingwell for handling our manuscript and K.-U. Hess for the fruitful review which helped to improve the quality of the manuscript.

References:

Adam, G., Gibbs, J.H., 1965. On the temperature dependence of cooperative relaxation properties in glass-forming liquids. J. Chem. Phys. 43, 139-146.

Baasner, A., Schmidt, B.C., Webb, S.L., 2013. The effect of chlorine, fluorine and water on the viscosity of aluminosilicate melts. Chem. Geol. 357, 134-149.

ACCEPTED MANUSCRIPT

Baker, D.R., Moretti, R., 2011. Modeling the solubility of sulfur in magmas: a 50-year old geochemical challenge. In: H. Behrens and J.D.Webster (eds.) Sulfur in magmas and melts: Its importance for natural and technical processes. Washington, Mineralogical Society of America, Geochemical Society, Reviews in Mineralogy and Geochemistry 73, 167-213.

Botcharnikov, R.E., Behrens, H., Holtz, F., Koepke, J., Sato, H., 2004; Sulfur and chlorine solubility in Mt. Unzen rhyodacitic melt at 850 °C and 200 MPa. Chem. Geol. 213, 207-225.

Brandiss, M.E., Stebbins, J.F., 1988. Effects of T on the structures of silicate liquids: ^{29}Si NMR results. Geochim. Cosmochim. Acta 52, 2659-2669.

Carroll, M.R., Rutherford, M.J., 1988. Sulfur speciation in hydrous experimental glasses of varying oxidation state: Results from measured wavelength shifts of sulfur X-rays. Am. Mineral. 73, 845-849.

Carroll, M.R., Webster, J.D., 1994. Solubilities of sulfur, noble gases, nitrogen, chlorine, and fluorine in magmas. In: J.R. Holloway and M.R. Carroll. (eds.) Volatiles in Magmas. Washington, Mineralogical Society of America, Geochemical Society, Reviews in Mineralogy 30, 231-280.

ACCEPTED MANUSCRIPT

Clemente, B., Scaillet, B., Pichavant, M., 2004. The solubility of sulfur in hydrous rhyolitic melts. J. Petrol. 45, 2171-2196.

De Hoog, J.C.M., Mason, P.R.D., van Bergen, M.J., 2001. Sulfur and chalcophile elements in subduction zones: Constraints from a laser ablation ICP-MS study of melt inclusions from Galunggung Volcano, Indonesia. Geochim. Cosmochim. Acta 65, 3147-3164.

Deubener, J., Muller, R., Behrens, H., Heide, G., 2003. Water and the glass transition temperature of silicate melts. J. Non-Cryst. Solids 330, 268-273.

Di Carlo, I., Pichavant, M., Rotolo, S.G., Scaillet, B., 2006. Experimental crystallization of a high-K arc basalt: The golden pumice, Stromboli volcano (Italy). J. Petrol. 47, 1317-1343.

Di Genova, D., Romano, C., Hess, K.-U., Vona, A., Poe, B.T., Giordano, D., Dingwell, D.B., Behrens, H., 2013. The rheology of peralkaline rhyolites from Pantelleria Island. J. Volc. Geotherm. Res. 249, 201-216.

Dingwell, D.B., 1995. Relaxation in silicate melts: some applications. In: Stebbins J.F, McMillan P.F. and Dingwell D.B. (eds) Structure, dynamics and properties of silicate melts. Washington, Mineralogical Society of America, Geochemical Society, Reviews in Mineralogy 32, pp 21-66.

ACCEPTED MANUSCRIPT

Dingwell, D.B., Romano, C., Hess, K.-U., 1996. The effect of water on the viscosity of a haplogranitic melt under P-T-X conditions relevant to silicic volcanism. Contrib. Mineral. Petrol. 124, 19-28.

Dingwell, D.B., Hess, K.-U., Romano, C., 1998. Viscosity data for hydrous peraluminous granitic melts: Comparison with a metaluminous model. Am. Mineral. 83, 236-239.

Edmonds, M., Oppenheimer, C., Pyle, D.M., Herd, R.A., Thompson, G., 2003. SO_2 emissions from Soufriere Hills Volcano and their relationship to conduit permeability, hydrothermal interaction and degassing regime. J. Volc. Geotherm. Res. 124, 23-43.

Farnan, I., Kohn, S.C., Dupree, R., 1987. A study of the structural role of water in hydrous silica glass using Cross-Polarization Magic Angle Spinning NMR. Geochim. Cosmochim. Acta 51, 2869-2873.

Fincham, C.J.B., Richardson, F.D., 1954. The behavior of sulfur in silicate and aluminate melts. Proc. Royal Soc. London A 223, 40-62.

Frantz, J.D., Mysen, B.O., 1995. Raman spectra and structure of $BaO-SiO_2$, $SrO-SiO_2$ and $CaO-SiO_2$ melts to 1600°C. Chem. Geol. 121, 155-176.

ACCEPTED MANUSCRIPT

Freda, C., Baker, D.R., Scarlato, P., 2005. Sulfur diffusion in basaltic melts. Geochim. Cosmochim. Acta 69, 5061-5069.

Giordano, D., Dingwell, D.B., 2003. Non-Arrhenian multicomponent melt viscosity: A model. Earth Planet. Science Lett. 208, 337-349.

Giordano, D., Romano, C., Poe, B., Dingwell, D.B., Behrens, H., 2004. The combined effects of water and fluorine on the viscosity of silicic magmas. Geochim. Cosmochim. Acta 68, 5159-5168.

Giordano, D., Nichols, A.R.L., Dingwell, D.B., 2005. Glass transition temperatures of natural hydrous melts: a relationship with shear viscosity and implications for the welding process. J. Volc. Geotherm. Res. 142, 105-118.

Giordano, D., Potuzak, M., Romano, C., Dingwell, D.B., Nowak, M., 2008a. Viscosity and glass transition temperature of hydrous melts in the system $CaAl_2Si_2O_8$–$CaMgSi_2O_6$. Chemical Geology 256, 203-215.

Giordano, D., Russell, J.K., Dingwell, D.B., 2008b. Viscosity of magmatic liquids: A model. Earth Planet. Science Lett. 271, 123-134.

ACCEPTED MANUSCRIPT

Grimmer, A.R., Magi, M., Hähnert, M., Stade, H., Samoson, A., Wieker, W., Lippmaa, E., 1984. High resolution solid state ^{29}Si NMR spectroscopic studies of binary alkali silicate glasses. Phys. Chem. Glasses 25, 105-109.

Hess, K.U., Dingwell, D.B., 1996. Viscosities of hydrous leucogranitic melts: a non-Arrhenian model. Am. Mineral. 81, 1297-1300.

Jugo, P.J., Luth, R.W., Richards, J.P., 2005a. An experimental study of the sulfur content in basaltic melts saturated with immiscible sulfide or sulfate liquids at 1300°C and 1.0 GPa. J. Petrol. 46, 783-798.

Jugo, P.J., Luth, R.W., Richards, J.P., 2005b. Experimental data on the speciation of sulfur as a function of oxygen fugacity in basaltic melts. Geochim. Cosmochim. Acta 69, 497-503.

Klimm, K., Botcharnikov, R.E., 2010. The determination of sulfate and sulfide species in hydrous silicate glasses using Raman spectroscopy. Am. Mineral. 95, 1574-1579.

Klimm, K., Kohn, S.C., O'Dell, L.A., Botcharnikov, R.E., Smith, M.E., 2012a. The dissolution mechanism of sulphur in hydrous silicate melts. I: Assessment of analytical

ACCEPTED MANUSCRIPT

techniques in determining the sulphur speciation in iron-free to iron-poor glasses. Chem. Geol. 322-323, 237-249

Kummerlen, J., Merwin, L.H., Sebald, A., Keppler, H., 1992. Structural role of H_2O in sodium silicate glasses: results from ^{29}Si and ^{1}H NMR spectroscopy. J. Phys. Chem. 96, 6405-6410.

Liu, S.B., Stebbins, J.F., Schneider, E., Pines, A., 1988. Diffusive motion in alkali silicate melts: an NMR study at high temperature. Geochim. Cosmochim. Acta 52, 527-538.

Machacek, J., Gedeon, O., Liska, M., Marhoul, F., 2010. Molecular simulations of silicate melts doped with sulphur and nitrogen. J. Non-Cryst. Solids 356, 2458-2464.

Maekawa, H., Maekawa, T., Kawamura, S., Yokokawa, T., 1991. The structural groups of alkali silicate glasses determined from ^{29}Si MAS-NMR. J. Non-Cryst. Solids 127, 53-64.

Malfait, W.J., Xue, X., 2014. Hydroxyl speciation in felsic magmas. Geochim. Cosmochim. Acta 140, 606-620.

ACCEPTED MANUSCRIPT

ACCEPTED MANUSCRIPT

Malfait, W.J., Halter, W.E., Morizet, Y., Meier, B.H., Verel, R., 2007. Structural control on bulk melt properties: Single and double quantum 29Si NMR spectroscopy on alkali-silicate glasses. Geochim. Cosmochim. Acta 71, 6002-6018.

Manara, D., Grandjean, A., Pinet, O., Dussossoy, J.L., Neuville, D.R., 2007. Sulfur behavior in silicate glasses and melts: Implications for sulfate incorporation in nuclear waste glasses as a function of alkali cation and V_2O_5 content. J. Non-Cryst. Solids 353, 12-23.

Matjuschkin, V., Brooker, R.A., Tattitch, B., Blundy, J.D., Stamper, C.C., 2015. Control and monitoring of oxygen fugacity in piston-cylinder experiments. Contrib. Mineral. Petrol. 169, DOI 10.1007/s00410-015-1105-z.

Mazurin, O.V., 2007. Problems of compatibility of the value of glass transition temperatures published in the world literature. Glass Phys. Chem. 33, 22-36.

Merzbacher, C.I., Sherriff, B.L., Hartman, J.S., White, W.B., 1990. A high-resolution ^{29}Si and ^{27}Al NMR study of alkaline earth aluminosilicate glasses. J. Non-Cryst. Solids 124, 194-206.

Métrich, N., Clocchiatti, R., 1996. Sulfur abundance and its speciation in oxidized alkaline melts. Geochim. Cosmochim. Acta 60(21), 4151-4160.

ACCEPTED MANUSCRIPT

Métrich, N., Mandeville, C.W., 2010. Sulfur in magmas. Elements 6, 81-86.

Moretti, R., Ottonello, G., 2005. Solubility and speciation of sulfur in silicate melts: The Conjugated Toop-Samis-Flood-Grjotheim (CTSFG) model. Geochim. Cosmochim. Acta 69, 801-823.

Morizet, Y., Nichols, A.R.L., Kohn, S.C., Brooker, R.A., Dingwell, D.B., 2007. The influence of H_2O and CO_2 on the glass transition temperature: insights into the effects of volatiles on magma viscosity. Eur. J. Min. 19, 657-669.

Morizet, Y., Paris, M., Di Carlo, I., Scaillet, B., 2013. Effect of sulfur on the structure of silicate melts under oxidising conditions. Chem. Geol. 358, 131-147.

Morizet, Y., Vuilleumier, R., Paris, M., 2015. A NMR and molecular dynamics study of CO_2-bearing basaltic melts and glasses. Chem. Geol. *in press*.

Moune, S., Holtz, F., Botcharnikov, R.E., 2009. Sulphur solubility in andesitic to basaltic melts: Implications for Hekla volcano. Contrib. Mineral. Petrol. 157, 691-707.

ACCEPTED MANUSCRIPT

Moynihan, C.T., 1995. Relaxation in silicate melts: some applications. In: J. Stebbins, P.F. McMillan and D.B. Dingwell. (eds.) Structure, dynamics and properties of silicate melts. Washington, Mineralogical Society of America, Geochemical Society Reviews in Mineralogy 32, 1-20.

Moynihan, C.T., Easteal, A.J., DeBolt, M.A., Tucker, J., 1976. Dependence of fictive temperature of glass on cooling rate. J. Am. Ceram. Soc. 59, 12-16.

Mysen, B.O., 1988. Structure and properties of silicate melts. In: Development in Geochemistry, vol. 4. Elsevier, Amsterdam, 354 pp.

Mysen, B.O., 1990. Effect of pressure, temperature and bulk composition on the structure and species distribution in depolymerised alkali aluminosilicate melts and quenched melts. J. Geophys. Res. B 95, 15733-15744.

Mysen, B.O., Frantz, J.D., 1993. Structure and properties of alkali silicate melts at magmatic temperature. Eur. J. Min. 5, 393-407.

Mysen, B.O., Richet, P., 2005. Silicate glasses and melts: Properties and structure. pp. 560.

ACCEPTED MANUSCRIPT

ACCEPTED MANUSCRIPT

Mysen, B.O., 1998. Transport and configurational properties of silicate melts: Relationship to melt structure at magmatic temperatures. Phys. Earth and Planet. Int. 107, 23-32.

Mysen, B.O., Cody, G.D., 2005. Solution mechanisms of H_2O in depolymerized peralkaline melts. Geochim. Cosmochim. Acta 69, 5557-5566.

Mysen, B.O., Virgo, D., Scarfe, C.M., 1980. Relations between the anionic structure and viscosity of silicate melts – a Raman spectroscopic study. Am. Mineral. 65, 690-710.

Nagashima, S., Katsura, T., 1973. The solubility of S in Na_2O–SiO_2 melts under various oxygen partial pressures at 1100°C, 1250°C, and 1300°C. Bull. Chem. Soc. Japan 46, 3099-3103.

Neuville, D.R., 2006. Viscosity, structure and mixing in (Ca, Na) silicate melts. Chem. Geol. 229, 28-41.

O'Neill, H.S.C., Mavrogenes, J.A., 2002. The sulfide capacity and the sulfur content at sulfide saturation of silicate melts at 1400°C and 1 bar. J. Petrol. 43, 1049-1087.

Oppenheimer, C., Scaillet, B., Martin, R.S., 2011. Sulfur degassing from volcanoes: source conditions, surveillance, plume chemistry and Earth system impacts. Sulfur in magmas and

ACCEPTED MANUSCRIPT

melts: Its importance for natural and technical processes. H. Behrens and J. D. Webster. Washington, Mineralogical Society of America, Geochemical Society Reviews in Mineralogy and Geochemistry 73, 363-421.

Paris, E., Giuli, G., Carroll, M.R., Davoli, I., 2001. The valence and speciation of sulfur in glasses by X-ray absorption spectroscopy. Can. Mineral. 39, 331-339.

Py, X., Calvet, N., Olives, R., Meffre, A., Echegut, P., Bessada, C., Veron, E., Ory, S., 2011. Recycled material for sensible heat based thermal energy storage to be used in concentrated solar thermal power plants. J. Solar Ener. Eng. 133, doi:10.1115/1.4004267.

Richet, P., Lejeune, A.-M., Holtz, F., Roux, J., 1996. Water and the viscosity of andesite melts. Chem. Geol. 128, 185-197.

Robert, G., Whittington, A.G., Stechern, A., and Behrens, H., 2013. The effect of water on the viscosity of a synthetic calc-alkaline basaltic andesite. Chem. Geol. 346, 135-148.

Robert, G., Whittington, A.G., Stechern, A., and Behrens, H., 2014. Heat capacity of hydrous basaltic glasses and liquids. J. Non-Cryst. Solids 390, 19-30.

ACCEPTED MANUSCRIPT

Romano, C., Poe, B., Mincione, V., Hess, K.-U., Dingwell, D.B., 2001. The viscosities of dry and hydrous XAlSi3O8 (X = Li, Na, K, Ca0.5, Mg0.5) melts. Chem. Geol. 174, 115-132.

Scaillet, B., Holtz, F., Pichavant, M., Schmidt, M., 1996. Viscosity of Himalayan leucogranites: Implications for mechanisms of granitic magma ascent. J. Geophys. Res. B 101, 27691-27699.

Scaillet, B., Luhr, J.F., Carroll, M.C., 2003. Petrological and volcanological constraints on volcanic sulphur emissions to the atmosphere. Volcanism and the Earth's atmosphere. A. Robock and C. Oppenheimer. Geophys. Mono. 139, 11-40.

Scaillet, B., Pichavant, M., 2005. A model of sulphur solubility for hydrous mafic melts: application to the determination of magmatic fluid compositions of Italian volcanoes. Ann. Geophys. 48(4/5), 671-697.

Spillaert, N., Métrich, N., Allard, P., 2006. S-Cl-F degassing pattern of water-rich alkali basalt: Modelling and relationship with eruption styles on Mount Etna volcano. Earth Planet. Science Lett. 248, 772-786.

Stebbins, J.F., 1995. Dynamics and structure of silicate and oxide melts: Nuclear Magnetic Resonance studies. J.F. Stebbins, P.F. McMillan and D.B. Dingwell. Washington, Mineralogical Society of America, Geochemical Society 32, 190-246.

ACCEPTED MANUSCRIPT

Toplis, M.J., Dingwell, D.B., 2004. Shear viscosities of CaO-Al_2O_3-SiO_2 and MgO-Al_2O_3-SiO_2 liquids: Implications for the structural role of aluminium and the degree of polymerisation of synthetic and natural aluminosilicate melts. Geochim. Cosmochim. Acta 68, 5169-5188.

Webb, S.L., Dingwell, D.B., 1990. Non-Newtonian rheology of igneous melts at high stresses and strain rates: Experimental results for rhyolite, andesite, basalt and nephelinite, J. Geophys. Res., 95, 15695–15701.

Webster J.D., Mandeville, C.W., 2007. Fluid immiscibility in volcanic environments. Rev Mineral Geochem. 65, 313-362.

Whittington, A., Richet, P., Holtz, F., 2000. Water and the viscosity of depolymerized aluminosilicate melts. Geochim. Cosmochim. Acta 64, 3725-3736.

Whittington, A., Richet, P., Linard, Y., Holtz, F., 2001. The viscosity of hydrous phonolites and trachytes. Chem. Geol. 174, 209-223.

ACCEPTED MANUSCRIPT

Xue, X., Kanzaki, M., 2004. Dissolution mechanisms of water in depolymerized silicate melts: Constraints from 1H and 29Si NMR spectroscopy and ab intio calculations. Geochim. Cosmochim. Acta 68, 5027-5057.

Xue, X., Kanzaki, M., 2008. Structure of hydrous aluminosilicate glasses along the diopside-anorthite join: A comprehensive one- and two-dimensional 1H and 27Al NMR study. Geochim. Cosmochim. Acta 72, 2331-2348.

Xue, X., 2009. Water speciation in hydrous silicate and aluminosilicate glasses: Direct evidence from 29Si-1H and 27Al-1H double-resonance NMR. Am. Mineral. 94, 395-398.

Zajacz, Z., 2015. The effect of melt composition on the partitioning of oxidized sulfur between silicate melts and magmatic volatiles. Geochim. Cosmochim. Acta, *in press*.

Zeng, Q., Nekvasil, H., Grey, C.P., 1999. Proton environments in hydrous aluminosilicate glasses: A 1H MAS, 1H/27Al, and 1H/23Na TRAPDOR NMR study. J. Phys. Chem. B 103, 7406-7415.

Zotov, N., Keppler, H., 1998. The influence of water on the structure of hydrous sodium tetrasilicate glasses. Am. Mineral. 83, 823-834.

ACCEPTED MANUSCRIPT

Figure caption:

Figure 1: A) Tg determination from the three point tangent definition on AD-5-3. B) Replicated DSC measurements for AD-5-3 using different heating rate: 10 or 20 K/min. The determination of Tg appears easier for measurements with 20 K/min due to the more important decrease in the heat flow value across the glass transition region. Above Tg, heat flow curve is strongly affected by crystallization processes around 700°C.

Figure 2: Combined DSC and TGA measurements for AD-5-0 (A) and AD-5-1 (B). A significant weight loss (in %) occurs well above Tg suggesting that the Tg determination is not affected by potential diffusive loss of S or H_2O escaping the sample powder.

Figure 3: Typical DSC curves obtained for several samples. The curve are not placed as a function of volatile content but one can appreciate the change in Tg value with varying volatile content indicated in between brackets (ppm S,wt.%H_2O).

Figure 4: A) Change in Tg as a function of wt.% H_2O. The Tg value decreases with increasing water content following an exponential decay function (solid curve calculated with Eq. 3). We show the change in Tg as a function of wt.% H_2O for a theoretical anorthite-diopside eutectic glass composition calculated with the models of Giordano et al. (2008a,b) (dashed and dotted curves). B) Change in Tg value as a function of ppm S. The reported volatile content was determined with micro-FTIR for wt.% H_2O and EPMA for ppm S. There is no identifiable trend between Tg value and the ppm S suggesting that the effect of S on Tg is limited. We added the expected Tg value at a given H_2O content (2.0 to 4.0 wt.%). At a

ACCEPTED MANUSCRIPT

given wt.% H_2O, a S-bearing sample will exhibit a lower Tg value than expected by the calculation with Eq. 3.

Figure 5: Calculated Tg versus Measured Tg. Tg is calculated with the model of Giordano et al. (2008a) (A) and with the empirical Eq. 2. The Tg values are reproduced within ±19°C with Eq. 2. The error on Tg with the model of Giordano et al. (2008a) is assumed to be ±2.5°C.

Table caption:

Table 1: Sample dataset, experimental conditions, volatile content and speciation.

Table 2: Differential Scanning Calorimetry results.

ACCEPTED MANUSCRIPT

ACCEPTED MANUSCRIPT

Figure 1

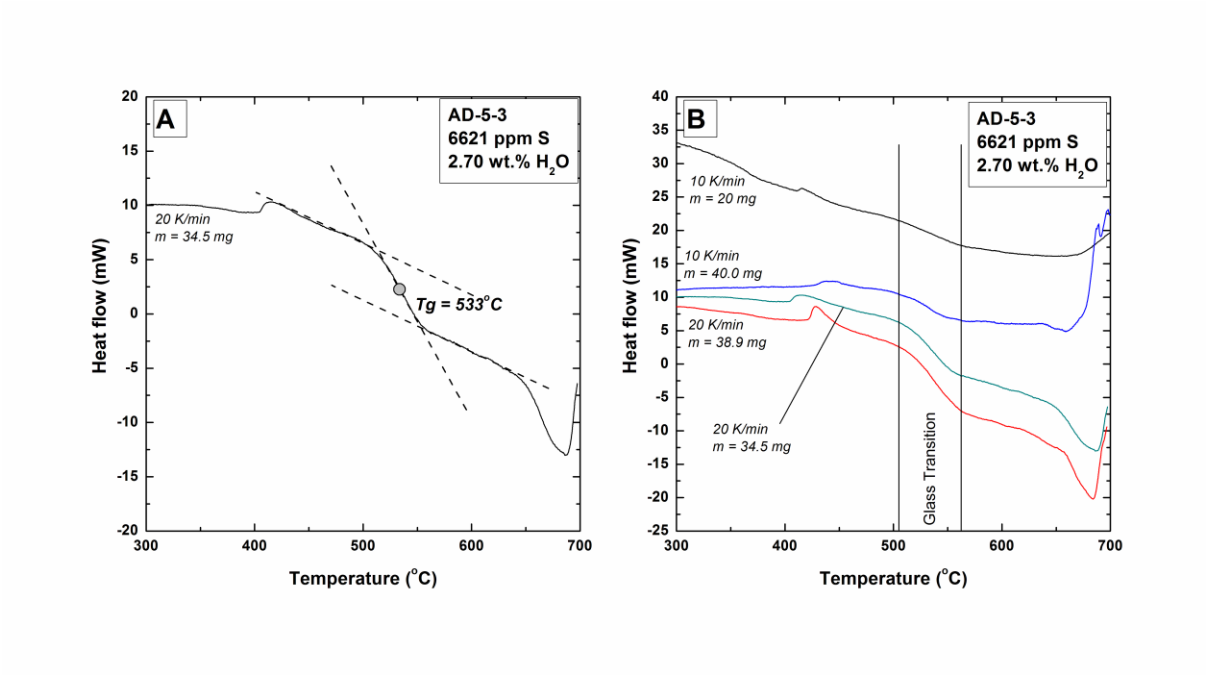

ACCEPTED

ACCEPTED MANUSCRIPT

Figure 2

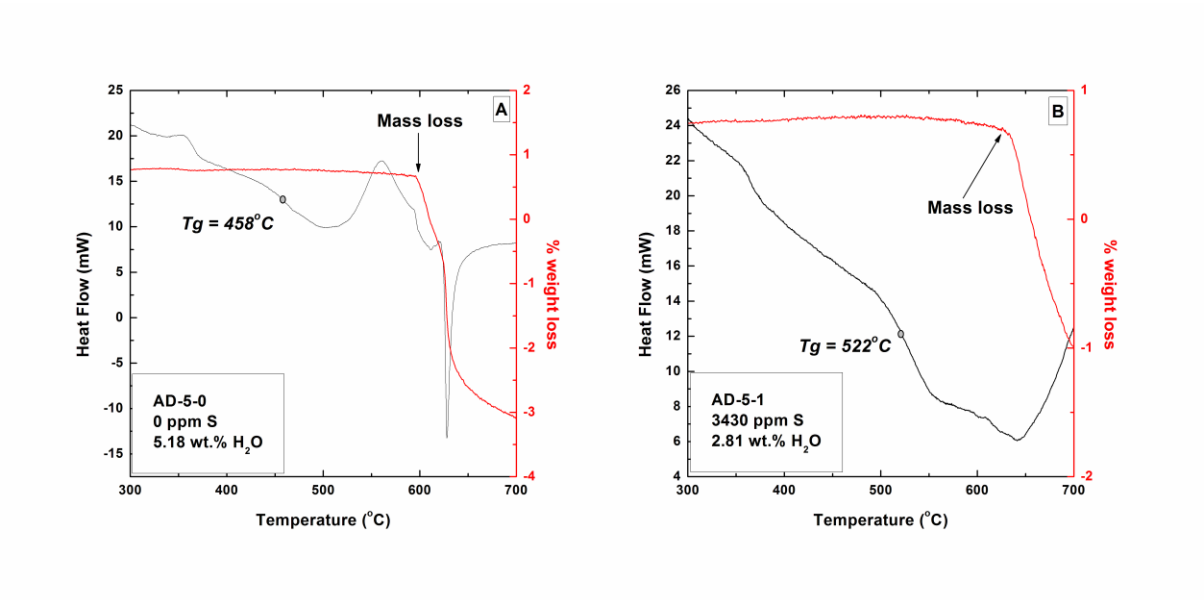

ACCEPTED MANUSCRIPT

ACCEPTED MANUSCRIPT

Figure 3

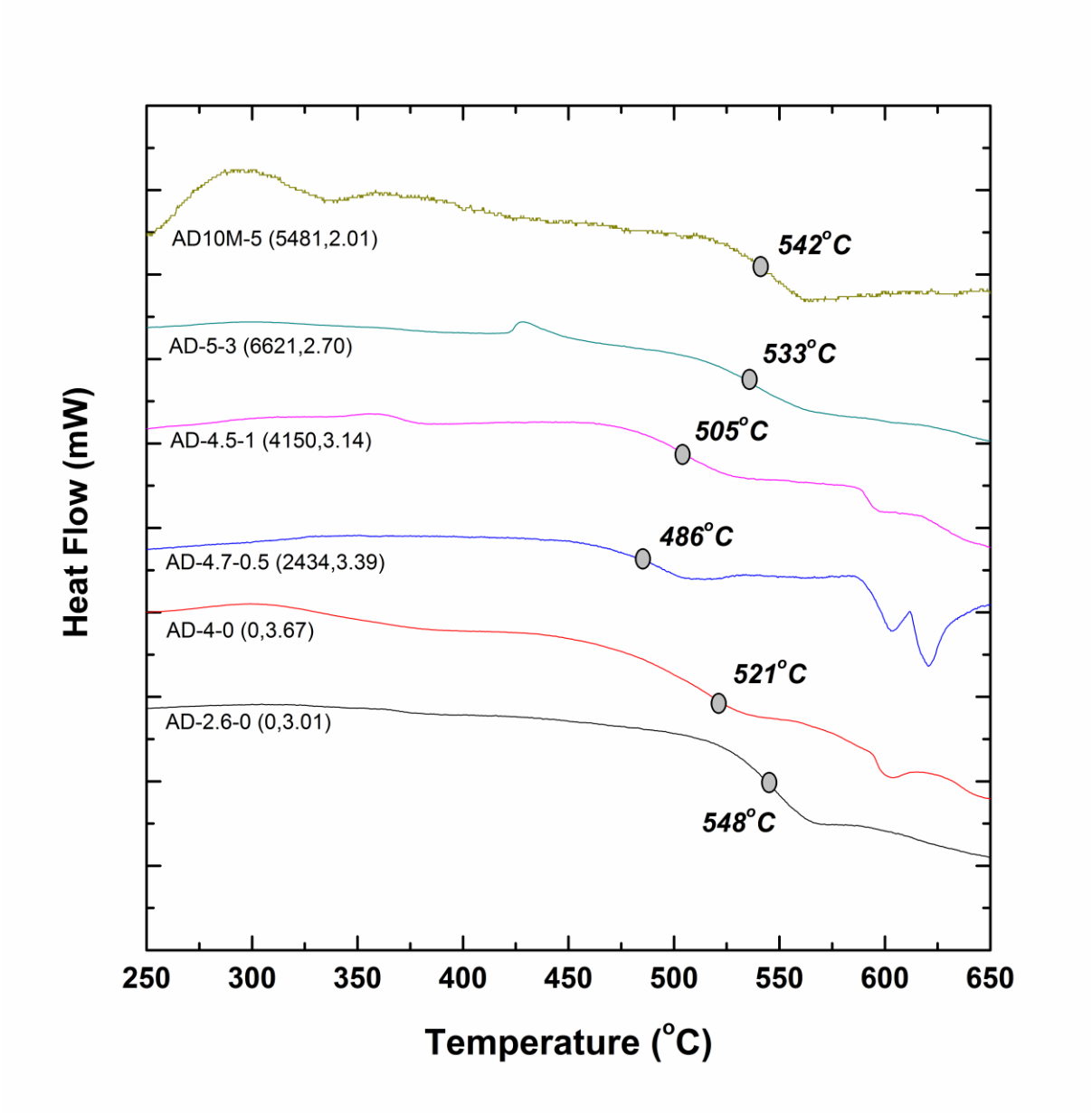

ACCEPTED MANUSCRIPT

Figure 4

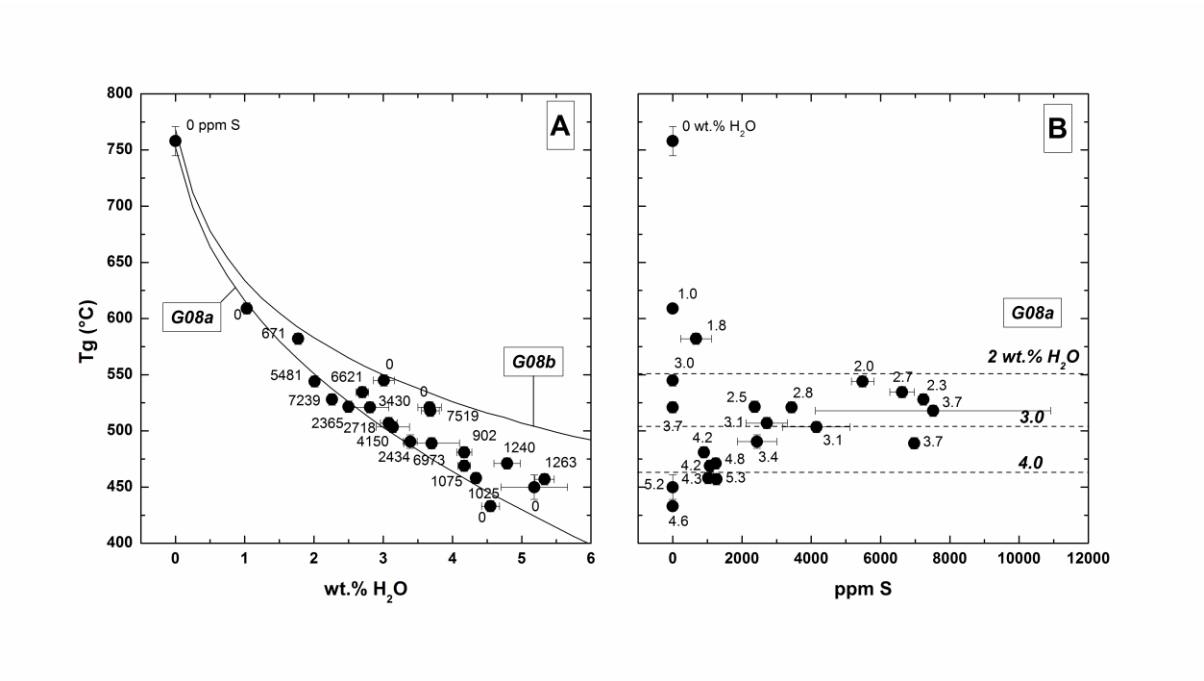

ACCEPTED

ACCEPTED MANUSCRIPT

Figure 5

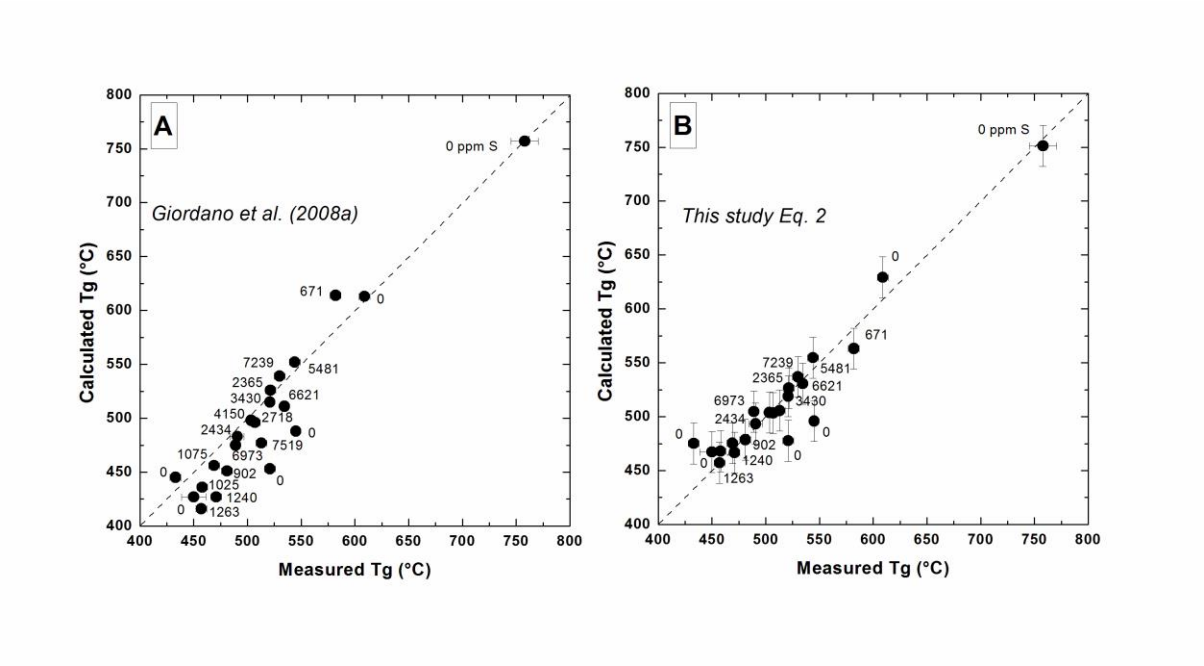

ACCEPTED MANUSCRIPT

ACCEPTED MANUSCRIPT

Table 1

Samples	Experimental conditions					ppm S[a]	S speciation[c]		wt.% H_2O[b]
	Pressure (MPa)	Temperature (°C)	Log fO_2 (ΔFMQ)[d]	Loaded S (wt.%)	Loaded H_2O (wt.%)		XSO_4^{2-}	XHS^-	
ADVF	0.001	1400	+5	0	0	0	0	0	0
AD1H-6[e]	500	1450	>+1	0	1.2	0	0	0	1.03 (0.03)
AD2H-6[e]	500	1450	>+1	0	8.2	0	0	0	4.55 (0.13)
AD-5-0	300	1250	+2.8	0	4.9	0	0	0	5.18 (0.48)
AD-3-0	300	1250	+2.8	0	2.6	0	0	0	3.01 (0.15)
AD-4-0	300	1250	+2.8	0	3.9	0	0	0	3.67 (0.17)
AD-4.7-0.5	300	1250	+2.8	0.5	4.7	2434 (567)	1	0	3.39 (0.10)
AD-5-1	300	1250	+1.9	1.0	4.8	3430 (136)	1	0	2.81 (0.27)
AD-4.5-1	300	1250	+2.1	1.0	4.6	4150 (974)	1	0	3.14 (0.24)
AD-5-3	300	1250	+1.8	3.0	4.7	6621 (355)	1	0	2.70 (0.09)
AD-5-5	300	1250	+2.3	5.0	4.9	7519 (3397)	0.97	0.03	3.68 (0.13)
AD4	300	1250	+2.0	0.25	4.6	2718 (598)	1	0	3.08 (0.12)
AD10	300	1250	+2.3	4.9	7.2	6973 (73)	1	0	3.70 (0.43)
AD12	300	1250	+1.2	5.1	2.2	671 (441)	1	0	1.77 (0.04)
AD20	300	1250	+2.1	1.1	5.2	1240 (25)	0.99	0.01	4.79 (0.19)
AD21	300	1250	+1.9	0.5	4.4	902 (26)	0.99	0.01	4.17 (0.11)
AD22	300	1250	+1.9	0.2	5.0	1025 (20)	0.99	0.01	4.34 (0.04)
AD23	300	1250	+1.2	1.0	5.5	1263 (91)	0.98	0.02	5.33 (0.14)
AD24	300	1250	+0.8	0.6	4.8	1075 (59)	0.98	0.02	4.17 (0.09)
AD5M-2[e]	500	1450	>+1	0.7	2.6	7239 (90)	1	0	2.26 (0.05)
AD2M-5[e]	500	1450	>+1	0.25	3.5	2365 (138)	1	0	2.50 (0.04)
AD10M-5[e]	500	1450	>+1	1.6	3.2	5481 (324)	1	0	2.01 (0.04)

[a] The S content is reported in Morizet et al. (2013) and has been determined via EPMA measurements. More than 20 spots were taken on each glass sample to obtain the standard deviation (numbers between brackets).

[b] The wt.% H_2O was determined with micro-FTIR measurements on doubly polished plate. Three to five spectra were taken for standard error determination.

[c] The S speciation was determined with Raman spectroscopy (see Supplementary material for typical Raman spectra). The HS^- contribution (peak located at 2575 cm^{-1}) is small and does not exceed 3% of the total S.

[d] The log fO_2 has been calculated using the total H_2O content and is reported relative Fayalite – Magnetite – Quartz (FMQ) buffer.

ACCEPTED MANUSCRIPT

[e] Those samples were synthesised using piston-cylinder apparatus at 500 MPa. In the S-bearing experiments, the S was loaded prior the experiment in the Pt capsule as H_2SO_4 aqueous solution of 2, 5 and 10 $mol.L^{-1}$ in concentration.

ACCEPTED MANUSCRIPT

ACCEPTED MANUSCRIPT

Table 2

Samples	DSC analytical conditions				Tg from Giordano et al. (2008a): H_2O effect[b]	Tg from Eq. 2: H_2O and S effects
	m (mg)	heating rate (K/min)	Tg (°C)	Average Tg (°C)[a]		
ADVF	42.1	10	767	758 ±13	757 ±2.5	751 ±19
	82.2	10	749			
AD1H-6	23.9	10	609	609 ±5	613	629
AD2H-6	21.6	10	433	433 ±5	445	475
AD-5-0	43.8	10	458	450 ±11	427	467
	46.0	10	442			
AD-3-0	28.4	10	544	545 ±5	488	496
	41.3	20	548			
	27.4	10	543			
AD-4-0	82.5	20	521	521 ±5	453	478
AD-4.7-0.5	15.6	10	486	491 ±6	483	493
	21.3	10	495			
AD-5-1	41.0	10	522	521 ±5	515	519
	53.0	10	520			
AD-4.5-1	24.0	10	502	504 ±5	498	504
	39.0	20	505			
AD-5-3	20.0	10	538	535 ±5	511	506
	38.9	20	533			
	40.0	10	534			
	34.5	20	533			
AD-5-5	27.2	10	518	513 ±5	477	506
	36.5	10	510			
	44.7	10	511			
AD4	84.1	10	507	507 ±5	496	503
AD10	52.0	10	488	489 ±5	475	505
	32.6	10	490			
AD12	59.0	10	582	582 ±5	614	563
AD20	58.7	10	471	471 ±5	427	467
AD21	80.6	10	481	481 ±5	451	478
AD22	77.8	10	458	458 ±5	436	468
AD23	61.8	10	457	457 ±5	416	457
AD24	66.1	10	469	469 ±5	456	475
AD5M-2	39.4	10	528	530 ±5	539	537
	25.7	10	532			
AD2M-5	17.1	10	521	522 ±5	526	526
	9.0	10	522			
AD10M-5	16.3	10	542	544 ±5	552	555
	11.2	10	546			

[a] Tg was determined from the two tangents, three points methods (see text for details). The error corresponds to the standard deviation of the obtained from the replicated Tg measurements. In the case the standard deviation is low; we still apply a ±5°C as a standard error.

ACCEPTED MANUSCRIPT

[b] The model of Giordano et al. (2008a) is used to calculate a Tg value which is a function of the water content and takes into account the chemical composition determined by EPMA analyses (see Supplementary material). The error on Tg is the one reported for the model (±2.5).

ACCEPTED MANUSCRIPT

ACCEPTED MANUSCRIPT

Highlight

- Sulfate groups (SO_4^{2-}) do not affect glass transition temperature.
- Discrepant with spectroscopic observation.
- Limited effect of S on melt viscosity.

ACCEPTED MANUSCRIPT